Inorganic Chemistry

Communication

pubs.acs.org/IC

Anomalous Anisotropic Thermal Expansion in a One-Dimensional Coordination Polymer Driven by Conformational Flexibility

Raj Kumar Das, Himanshu Aggarwal, and Leonard J. Barbour*

Department of Chemistry and Polymer Science, University of Stellenbosch, Matieland, 7602 Stellenbosch, South Africa

Supporting Information

ABSTRACT: A one-dimensional lithium(I) coordination polymer has been characterized by variable-temperature single-crystal X-ray diffraction and differential scanning calorimetry. This compound possesses an anisotropic packing arrangement that, along with a scissor-like or hingelike movement of the pyridyl ligand side arms, results in an extremely rare combination of positive, negative, and zero thermal expansion. Designing such types of materials and understanding the mechanistic details can facilitate the design of new thermoresponsive materials.

Most three-dimensional materials expand along all three directions with increasing temperature, and the phenomenon is known as positive thermal expansion (PTE).[1] The mechanism for PTE involves longitudinal atomic vibrations that give rise to equilibrium interatomic distances that increase with temperature. For many common materials, the magnitude of linear thermal expansion (given by the coefficient α) is typically on the order of about 20 MK^{-1}.[2] However, in some instances, the thermal response is quite different; i.e., the increases in bond lengths are either counterbalanced or overshadowed by some other phenomenon (transverse vibrational motions,[3] INVAR effect,[4] etc.), giving rise to either zero (ZTE)[5] or negative linear thermal expansion (NTE),[6] respectively. Moreover, thermal expansion behavior can be either isotropic or anisotropic in nature. Isotropic NTE has been reported for materials having cubic symmetry, and examples include IRMOFs, HKUST-1, cyano-bridged metal−orgainc frameworks (MOFs), etc.[7] Owing to their inherently asymmetric packing (relative to cubic systems), noncubic materials generally exhibit anisotropic thermal expansion. If any material possesses one or more nonpositive linear thermal expansion coefficients, then the behavior is called anomalous thermal expansion. The most common types of anomalous thermal expansion occur as a result of lattice-fence or hingelike responses in helices, zigzag chains, and gridlike networks.[8] Such materials expand along one direction with concomitant contraction along perpendicular directions (or vice versa). Extraordinarily large linear thermal expansion coefficients (>100 MK^{-1}) have been reported for several materials such as (*S*,*S*)-octa-3,5-diyn-2,7-diol,[9] methanol monohydrate,[10] $Ag_3[Co(CN)_6]$,[11] Prussian blue analogues,[12] etc. In recent years, MOFs have emerged as a new class of materials possessing anomalous thermal expansion behavior.[7,11,12] Furthermore, very few MOFs have been reported to possess a unique combination of PTE, NTE, and ZTE as a result of either a hingelike[13] or a combined stretching−tilting[14] mechanism.

Herein, we report the anomalous thermal expansion behavior of a one-dimensional coordination polymer, $\{[Li(4\text{-pyc})(H_2O)_{0.5}]\cdot 0.5MeOH\}_n$ (**1**; 4-pyc = 4-pyridinecarboxylate; Scheme S1). This material has been synthesized according to a modified literature procedure.[15] Single-crystal X-ray diffraction (SCD) analysis reveals that **1** crystallizes in monoclinic space group *C*2/*c*, and its asymmetric unit contains one Li^+ ion, one 4-pyc^- ligand, half of a coordinated water molecule, and half of a noncoordinated, disordered MeOH molecule (Figure S1).

The carboxylate groups coordinate to the Li^+ ions in a chelating-bridging mode, whereas the water molecules coordinate in a bridging mode to generate a one-dimensional zigzag chain along the crystallographic *c* axis (Figure 1a). Each one-dimensional coordination chain has noncoordinated pyridyl units as side arms, which adopt staggered orientations along the chain axis (Figure S2). The nitrogen atoms of the pyridyl units

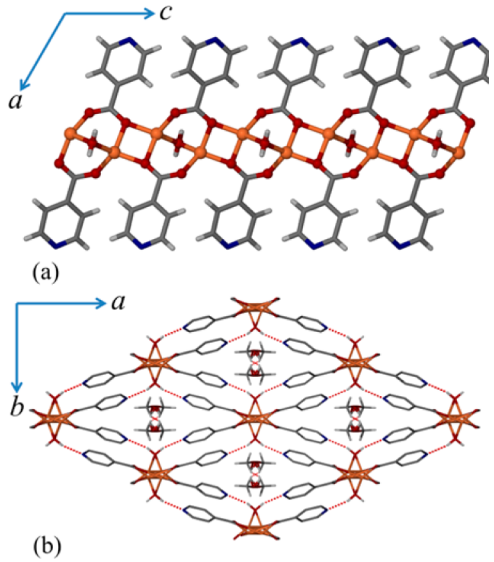

Figure 1. (a) Perspective view of a one-dimensional chain in **1** projected along [010] (lithium and oxygen atoms are shown in ball-and-stick representation, and all other atoms are shown as capped sticks). (b) Packing diagram viewed along the crystallographic *c* axis showing hydrogen-bonding interactions in **1** (aromatic hydrogen atoms are removed for clarity).

Received: July 13, 2015
Published: August 14, 2015

DOI: 10.1021/acs.inorgchem.5b01560
Inorg. Chem. 2015, 54, 8171−8173

form strong N−H···O hydrogen bonds (approximately along the crystallographic *a* axis) with the water molecules of neighboring chains to generate three-dimensional connectivity (Figure 1b).

The overall packing arrangement contains infinite one-dimensional solvent-accessible channels along [001] (with dimensions ∼4.6 × 12.4 Å, considering the contributions of the van der Waals radii of individual atoms), which are occupied by disordered MeOH molecules. Interestingly, the metal−ligand coordination bonds propagate along the crystallographic *c* axis and the hydrogen bonds along the *a* axis, whereas there are almost no notable interactions along the *b* axis. Owing to these directional discrepancies in interaction strength, the material possesses highly anisotropic geometrical flexibility along the three crystallographic axes. Inspired by this observation, we monitored the temperature-dependent structural changes using variable-temperature SCD.

X-ray intensity data were recorded at 20 K intervals in the temperature range of 100−260 K. The loss of crystal singularity above 260 K precluded further structural analysis. Over the temperature range investigated, the crystallographic *b* axis elongates significantly with increasing temperature, while the *a* axis shrinks and the *c* axis remains almost constant (Tables S1 and S2 and Figure S3). The crystallographic angle β also increases steadily with increasing temperature (Tables S1 and S2 and Figure S4). Because **1** crystallizes in the monoclinic crystal system, the program *PASCAL*[16a] was employed to calculate the orthogonal linear thermal expansion coefficients.

The linear thermal expansion coefficients along three principal thermal axes, X1 [0.6316, 0, 0.7753], X2 [−0.2763, 0, 0.9611], and X3 [0, 1, 0] are −42(2), 3(2), and 206(4) MK^{-1}, respectively (Figure 2). The material therefore exhibits the rare combination

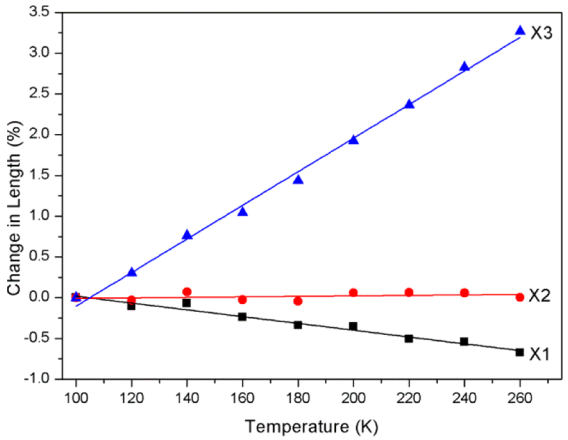

Figure 2. Plot of the temperature-dependent change in the principal tensor lengths (obtained from *PASCAL*).

of substantial NTE along X1, ZTE along X2, and colossal PTE along X3 (Figure S5). The volumetric thermal expansion coefficient of **1** is 169(5) MK^{-1} (Figure S6).

The reversibility of the expansion process was confirmed by determining the unit cell parameters after rapid cooling to 100 K, ramping to 260 K, and then cooling to 100 K again (100 K-R in the SI). The initial and final unit cell parameters are practically the same, and the crystal mosaicity also remains unaffected by temperature cycling.

The temperature-dependent structural changes have been examined carefully in order to elucidate the mechanism responsible for highly anisotropic thermal expansion of **1**. The metal−ligand coordination bonds are sufficiently strong to prevent any substantial change in the metal−metal nonbonding distances and the metal−oxygen−metal bridging angles (Table S3). This is consistent with ZTE along X2, which is approximately parallel to the crystallographic *c* axis. However, the thermal response in the *ab* plane is quite different, owing to conformational changes in the pyridyl side arms. With increasing temperature, the torsion angle N1···C2···C2′···N1′ (δ_1) increases steadily with a concomitant decrease in the torsion angle N1···C2···C2″···N1″ (δ_2) (Figures 3 and S7 and an SI

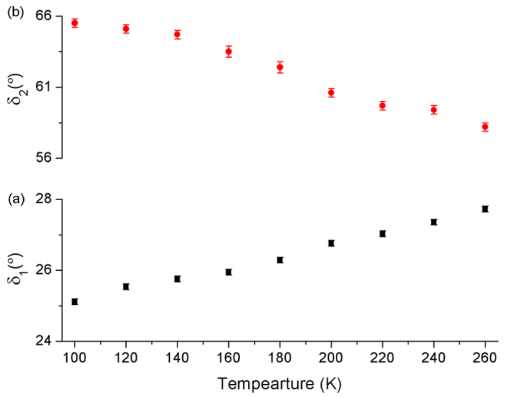

Figure 3. Variation of the torsion angles (a) δ_1 and (b) δ_2 with temperature.

video). As a result of these conformational changes, the noncovalent distance N1···N1′ along [0, 1, 0] (X3) becomes elongated (Table 1, Figures 4 and S8−S15, Table S4, and an SI

Table 1. Selected Noncovalent Distances in 1 Recorded at Different Temperatures

T (K)	N1···N1′ (Å)	N1···N1″ (Å)
100	6.086(3)	12.843(4)
140	6.121(3)	12.835(5)
180	6.147(3)	12.803(6)
220	6.189(3)	12.787(3)
260	6.227(3)	12.761(5)

video), resulting in PTE along that particular direction. Concurrently, the N1···N1″ distances along the *a* axis gradually

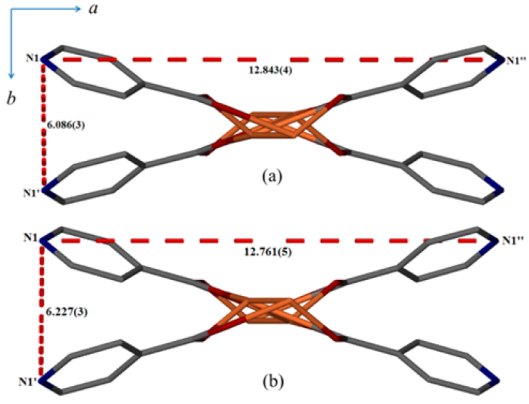

Figure 4. Perspective view showing selected noncovalent distances at (a) 100 and (b) 260 K (coordinated water molecules and hydrogen atoms are omitted for clarity).

DOI: 10.1021/acs.inorgchem.5b01560
Inorg. Chem. 2015, 54, 8171−8173

become shorter, thus contributing to the overall NTE along X1 (Table 1, Figures 4 and S8−S15, Table S4, and an SI video).

Interestingly, the N−H···O hydrogen-bonding interactions remain virtually unaffected during the entire thermal cycle (Table S5). Because **1** is more flexible along the *b* axis than along *a*, the magnitude of the PTE along X3 is greater than that of the NTE along X1. This observation is consistent with the notion that weaker and a lesser extent of intramolecular interactions in a particular direction would generally promote larger thermal expansion in that direction.[17] Differential scanning calorimetry (DSC) measurements rule out any possibility of a thermotropic phase transition because no thermal events are present (Figure S16) for the entire thermal cycle.

To date, all reports on the rare combination of PTE, NTE, and ZTE have involved either a hinged or a stretching−tilting motion of gridlike or macrocyclic units.[11,12] To the best of our knowledge, compound **1** is the first one-dimensional coordination polymer that exhibits such behavior. Moreover, the hingelike mechanism for structures containing one-dimensional chain motifs gives rise to substantial expansion along the chain axis.[8c,e,9] However, in the present report, **1** experiences a large extent of thermal expansion perpendicular to the chain axis without any significant expansion along the axis. The rigidity of the Li−O linkages results in ZTE along X2, whereas the conformational flexibility of the pyridyl side arms results in colossal PTE along X3 and substantial NTE along X1. Additionally, because the thermal expansion process occurs without affecting the crystal singularity, the precise temperature-dependent structural changes can be monitored in order to gain insight into the mechanism. Understanding such structure−property relationships can be propitious for developing new types of thermoresponsive materials for future applications.

■ ASSOCIATED CONTENT

Supporting Information

The Supporting Information is available free of charge on the ACS Publications website at DOI: 10.1021/acs.inorgchem.5b01560.

Synthetic procedure, DSC analysis, detailed crystallographic information, and additional figures (PDF)

Single-crystal data in CIF format (CIF)

An animation of the thermal expansion mechanism (AVI)

■ AUTHOR INFORMATION

Corresponding Author

*E-mail: ljb@sun.ac.za.

Notes

The authors declare no competing financial interest.

■ ACKNOWLEDGMENTS

We are grateful to the National Research Foundation and Department of Science and Technology (SARCHI Program) for financially supporting this work.

■ REFERENCES

(1) Ashcroft, N. W.; Mermin, N. D. *Solid State Physics*; Holt, Rinehart & Winston: New York, 1976.

(2) Krishnan, R. S.; Srinivasan, R.; Devanarayanan, S. *Thermal Expansion of Crystals*; Pergamon: Oxford, U.K., 1979.

(3) (a) Miller, W.; Smith, C. W.; Mackenzie, D. S.; Evans, K. E. *J. Mater. Sci.* **2009**, *44*, 5441−5451. (b) Lind, C. *Materials* **2012**, *5*, 1125−1154.

(4) (a) Guillaume, C. E. *CR Acad. Sci.* **1897**, *125*, 235−238. (b) Guillaume, C. E. *Nature* **1904**, *71*, 134−139. (c) van Schilfgaarde, M.; Abrikosov, I. A.; Johansson, B. *Nature* **1999**, *400*, 46−49.

(5) (a) Phillips, A. E.; Halder, G. J.; Chapman, K. W.; Goodwin, A. L.; Kepert, C. J. *J. Am. Chem. Soc.* **2010**, *132*, 10−11. (b) Margadonna, S.; Prassides, K.; Fitch, A. N. *J. Am. Chem. Soc.* **2004**, *126*, 15390−15391. (c) Song, X.; Sun, Z.; Huang, Q.; Rettenmayr, M.; Liu, X.; Seyring, M.; Li, G.; Rao, G.; Yin, F. *Adv. Mater.* **2011**, *23*, 4690−4694.

(6) (a) Peterson, V. K.; Kearley, G. J.; Wu, Y.; Ramirez-Cuesta, A. J.; Kemner, E.; Kepert, C. J. *Angew. Chem., Int. Ed.* **2010**, *49*, 585−588. (b) Goodwin, A. L.; Kepert, C. J. *Phys. Rev. B: Condens. Matter Mater. Phys.* **2005**, *71*, 140301−140304.

(7) (a) Wu, Y.; Kobayashi, A.; Halder, G. J.; Peterson, V. K.; Chapman, K. W.; Lock, N.; Southon, P. D.; Kepert, C. J. *Angew. Chem., Int. Ed.* **2008**, *120*, 9061−9064. (b) Goodwin, A. L.; Chapman, K. W.; Kepert, C. J. *J. Am. Chem. Soc.* **2005**, *127*, 17980−17981. (c) Dubbeldam, D.; Walton, K. S.; Ellis, D. E.; Snurr, R. Q. *Angew. Chem., Int. Ed.* **2007**, *46*, 4496−4499.

(8) (a) DeVries, L. D.; Barron, P. M.; Hurley, E. P.; Hu, C.; Choe, W. *J. Am. Chem. Soc.* **2011**, *133*, 14848−14851. (b) Goodwin, A. L. *Nat. Mater.* **2010**, *9*, 7−8. (c) Grobler, I.; Smith, V. J.; Bhatt, P. M.; Herbert, S. A.; Barbour, L. J. *J. Am. Chem. Soc.* **2013**, *135*, 6411−6414. (d) Engel, E. R.; Smith, V. J.; Bezuidenhout, C. X.; Barbour, L. J. *Chem. Commun.* **2014**, *50*, 4238−4241. (e) Jones, R. H.; Knight, K. S.; Marshall, W. G.; Clews, J.; Darton, R. J.; Pyatt, D.; Coles, S. J.; Horton, P. N. *CrystEngComm* **2014**, *16*, 237−243.

(9) (a) Das, D.; Jacobs, T.; Barbour, L. J. *Nat. Mater.* **2010**, *9*, 36−39. (b) Das, D.; Jacobs, T.; Pietraszko, A.; Barbour, L. J. *Chem. Commun.* **2011**, *47*, 6009−6011.

(10) Fortes, A. D.; Suard, E.; Knight, K. S. *Science* **2011**, *331*, 742−746.

(11) Goodwin, A. L.; Calleja, M.; Conterio, M. J.; Dove, M. T.; Evans, J. S. O.; Keen, D. A.; Peters, L.; Tucker, M. G. *Science* **2008**, *319*, 794−797.

(12) Goodwin, A. L.; Keen, D. A.; Tucker, M. G.; Dove, M. T.; Peters, L.; Evans, J. S. O. *J. Am. Chem. Soc.* **2008**, *130*, 9660−9661.

(13) (a) Henke, S.; Schneemann, A.; Fischer, R. A. *Adv. Funct. Mater.* **2013**, *23*, 5990−5996. (b) Zhou, H.-L.; Lin, R.-B.; He, C.-T.; Zhang, Y.-B.; Feng, N.; Wang, Q.; Deng, F.; Zhang, J.-P.; Chen, X.-M. *Nat. Commun.* **2013**, *4*, 2534.

(14) Lama, P.; Das, R. K.; Smith, V. J.; Barbour, L. J. *Chem. Commun.* **2014**, *50*, 6464−6467.

(15) Abrahams, B. F.; Dharma, A. D.; Grannas, M. J.; Hudson, T. A.; Maynard-Casely, H. E.; Oliver, G. R.; Robson, R.; White, K. F. *Inorg. Chem.* **2014**, *53*, 4956−4969.

(16) (a) Cliffe, M. J.; Goodwin, A. L. *J. Appl. Crystallogr.* **2012**, *45*, 1321−1329. (b) Belousov, R. I.; Filatov, S. K. *Glass Phys. Chem.* **2007**, *33*, 271−275. (c) Marmier, A.; Lethbridge, Z. A. D.; Walton, R. I.; Smith, C. W.; Parker, S. C.; Evans, K. E. *Comput. Phys. Commun.* **2010**, *181*, 2102−2115. (d) The *Win_strain* program is unpublished but available for download from www.rossangel.com.

(17) Kitaigorodsky, A. I. In *Molecular Crystals and Molecules*; Physical Chemistry Series No. 29; Loebl, E. M., Ed.; Academic Press: New York, 1973.

DOI: 10.1021/acs.inorgchem.5b01560
Inorg. Chem. 2015, 54, 8171−8173